Double-resonance determination of electron *g*-factors in muonium shallow-donor states

2004 J. Phys.: Condens. Matter 16 S4707

(http://iopscience.iop.org/0953-8984/16/40/015)

INSTITUTE OF PHYSICS PUBLISHING JOURNAL OF PHYSICS: CONDENSED MATTER

J. Phys.: Condens. Matter **16** (2004) S4707–S4720 PII: S0953-8984(04)85489-4

Double-resonance determination of electron g-factors in muonium shallow-donor states

J S Lord[1], S F J Cox[1,2,4], H V Alberto[3], J Piroto Duarte[3] and R C Vilão[3]

[1] ISIS Facility, Rutherford Appleton Laboratory, Chilton OX11 0QX, UK
[2] Department of Physics and Astronomy, University College London, WC1E 6BT, UK
[3] Physics Department, University of Coimbra, P-3004-516 Coimbra, Portugal

Received 2 April 2004
Published 24 September 2004
Online at stacks.iop.org/JPhysCM/16/S4707
doi:10.1088/0953-8984/16/40/015

Abstract

The discovery and significance of weakly bound muonium states with low hyperfine constants in a number of compound semiconductors of the II–VI and III–V (nitride) families are briefly reviewed. With ionization energies of several tens of meV, these imply that their hydrogen counterparts would act as shallow donors and that hydrogen could, either as an impurity or a deliberate dopant, be a source of electronic conductivity in the relevant materials. We examine whether, in their neutral undissociated states, the electron orbitals can be described in the effective-mass approximation and are correspondingly dilated, made up of conduction-band states. The best evidence that this is so comes from novel double-resonance measurements of the electron g-factors, devised for the ISIS pulsed muon source, and so far undertaken for ZnO, CdS, CdSe and CdTe. The respective values are $|g| = 1.97$, 1.86, 0.51 and 1.68; these results discount orbitally quenched compact states and are fully consistent with literature values for known shallow dopants in these compounds. They also illustrate the potential for μSR detection and characterization of such states in new electronic materials where hydrogen-induced conductivity is suspected or predicted.

1. Introduction

This paper presents muonium as a model for a certain class of hydrogen defect centre in semiconductors and dielectrics, namely the monatomic or isolated interstitial states of hydrogen impurity. In principle, these can be studied for hydrogen itself by ESR (electron spin resonance) and ENDOR (electron–nuclear double resonance) and we shall see that, for those materials where analogous states of hydrogen and muonium are known, μSR spectroscopy (in this context, muon spin rotation and resonance) gives essentially identical determinations of site

[4] Address for correspondence: ISIS Facility, Rutherford Appleton Laboratory, Chilton OX11 0QX, UK.

and electronic structure. In practice, muonium has been successfully characterized in a much wider range of semiconductors, both narrow-gap and wide-gap, than has hydrogen, giving a clearer picture of the systematics. This is in part due to the selectivity of μSR spectroscopy, and its high sensitivity *per spin*, but is chiefly due to its microsecond timescale, allowing detection of the isolated states before muonium encounters and reacts or pairs with other defects or impurities.

As for most such spectroscopic studies, particularly in chemistry or, as here, in chemical physics, this work exploits the concept of muonium as a light isotope of hydrogen. It relies on the expectation that the outcome (if not the speed) of any solid-state reaction will be identical for muonium and protium, at least in such simple binary compounds. This assumption applies to both stable and metastable configurations. The muonium–hydrogen analogy does not easily extend to kinetic or motional properties, such as rates of reaction, or of atomic or ionic diffusion. Here the isotopic mass ratio ($m_{\mathrm{Mu}}/m_{\mathrm{H}} \approx 1/9$) is often crucial, so that where protons or protium may be on the brink of the transition between classical and quantum diffusion, for muons and muonium the quantum aspects are invariably emphasized. Of course, for those interested in the diffusion of light interstitial defects, or in the classical to quantum transition more generally, muonium data are invaluable, providing a severe test of theoretical models. In an accompanying paper, we explore how the muonium–hydrogen analogy can be extended to the charge-state transitions and electrical activity of hydrogen [1]; in the present paper we confine our attention to sufficiently low (usually cryogenic) temperatures, where the charge and spin-states are sufficiently long lived to characterize electronic structure via hyperfine spectroscopy. For this purpose, one must be aware of the difference in zero-point energies and the correspondingly different spreads of the nuclear (i.e. muon and proton) wavefunctions, but these have minimal effect on the manner in which electronic structure is sampled via the observed hyperfine interactions.

Muonium centres in non-metals are now seen to fall into three reasonably distinct categories. The most numerous we call quasi-atomic, since they most closely resemble atomic muonium. Known in the early literature as 'normal muonium', they are the direct counterpart of the so-called trapped-atom states of interstitial hydrogen, known to ESR spectroscopy throughout the alkali halides as well as in a number of insulating oxides. Amongst these, the small variations of hyperfine constant for muonium and hydrogen, all within 10% of the respective free-atom values, show exactly the same systematics, offset by just a small zero-point energy correction [2]. Interestingly, the μSR studies of quasi-atomic muonium extend to the tetrahedrally coordinated semiconductors, where atomic hydrogen is not seen by ESR. Here we use the term 'quasi-atomic' advisedly, since the muonium hyperfine constants show a much wider variation in this family of materials—down to 45% of the free-atom value in silicon and even as low as 30% in the cuprous halides [3][5]. This indicates a corresponding degree of delocalization of the electron wavefunction onto the surrounding host atoms. In an LCAO description (linear combination of atomic orbitals), nonetheless, 1s(Mu) remains the leading and dominant term. This is illustrated by a sketch of unpaired electron density in figure 1(a); its value at the muon site itself determines the contact interaction which in these quasi-atomic states dominates the isotropic hyperfine constant. Recent compendia of muonium hyperfine constants extend to over thirty host materials [5, 6].

Also in certain tetrahedrally coordinated semiconductors, namely diamond, Si, Ge, GaAs and GaP, a second state of muonium is known. That is, muonium exhibits metastability in these materials: the hyperfine signature of the additional state coexists with that of quasi-atomic

[5] A similar result, namely 30% of the free-atom value, has most recently been measured for muonium in cuprous oxide, Cu_2O [4].

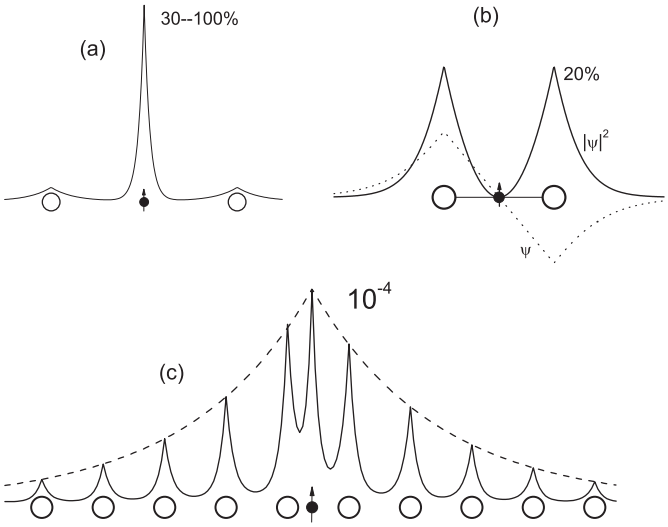

Figure 1. Sketches of unpaired electron density ($|\psi|^2$ ——) or LCAO depictions for (a) normal or quasi-atomic muonium, (b) bond-centred anomalous muonium or Mu* and (c) the putative shallow-donor states. The dotted curve in (b) (· · · · · ·) is the antisymmetric wavefunction (ψ) of the singly occupied orbital, emphasizing its nodal plane through the muon site. The dashed curve in (c) (- - - -) represents an envelope function with the form of a much dilated 1s orbital, with an effective Bohr radius given by equation (2).

muonium in the low-temperature spectra but indicates a quite different electronic structure [3]. Dubbed 'anomalous muonium' or Mu* in the early literature, it may be regarded as muonium which has reacted chemically with the host lattice, moving from an interstitial cage to the centre of a stretched bond [7]. In Si and diamond, at least, this may even be the more stable of the two states, although the question of their relative stability in Si is re-examined in an accompanying paper [1]. The bond-centred state has major spin density (of the unpaired electron, that is) located not on the muon but on the two adjacent host atoms of the stretched bond. Represented in figure 1(b), this makes the hyperfine interaction highly anisotropic and predominantly dipolar in character [7]. These two nearest neighbours together account for 40% of the spin density in Si, for example [8].

For bond-centred muonium in Si, Ge and diamond, the unpaired electron borrows a host antibonding orbital, depicted in figure 1(b), giving it donor character. The wavefunction itself (ψ as opposed to $|\psi|^2$) is perfectly antisymmetric about the muon site, so there can be no admixture of 1s(Mu), i.e. no atomic character at all. The singly occupied orbital has a node at the muon site and the contact interaction in these materials is in fact negative, representing spin polarization of the (doubly occupied) bonding or valence orbitals [7]. A small degree of 1s(Mu) occupancy becomes possible in GaAs and GaP, where the inversion symmetry is lost, so that the contact interaction then becomes a competition between positive and negative terms. This will also be the case in HgO, where we have discovered a muonium state with rather similar hyperfine parameters and binding energy to those of Mu* in Si [9, 10][6].

The point here is that normal (cage-centred) and anomalous (bond-centred) muonium both have fairly localized or compact electronic wavefunctions, albeit of quite different symmetry. They are both, in the nomenclature of semiconductor defects [11, 12], deep states. The binding or ionization energy of the electron, for bond-centred muonium in silicon, defines a donor level

[6] And likewise most recently in Ag_2O [4], though in neither Cu_2O nor Ag_2O do we yet have a muon site determination.

that lies several hundred meV below the conduction-band minimum [13]. The binding energy for cage-centred muonium cannot be measured directly but, given the hyperfine constants, must be a substantial fraction of a Rydberg, i.e. at least several electronvolts. Muonium in silica (quartz), for instance, remains unionized up to at least 1000 K [14].

In marked contrast with both normal and anomalous muonium is a third category of muonium states, discovered only recently, for which the ionization energies and temperatures are low and the hyperfine parameters are tiny (just several hundred kilohertz—lower by four orders of magnitude than the free-atom value). They have all the characteristics of the classic shallow-donor states exemplified, in silicon for instance, by impurities such as interstitial lithium or dopants such substitutional phosphorus. For such states, the paramagnetic electron of the unionized donor occupies a very much more extended orbital and is bound only weakly to the charge defect. At the time of writing, muonium states which appear to qualify for this shallow-donor category have been reported in CdS, CdSe, CdTe, ZnO, InN and, most recently, in GaN. That is, they occur in four of the II–VI compounds [15–18] and two of the III–Vs [19–21]. (Two other candidates seem likely, namely HgS and CdO, but remain to be confirmed [4, 22].)

Within the II–VIs, these apparently shallow states contrast with the quasi-atomic muonium states in ZnS and ZnSe that were reported summarily in the early μSR literature [3] and have recently been characterized more fully [23]. They likewise contrast with the deep-donor state lately found in HgO [9, 10]. In the III–Vs, the coexisting normal and anomalous muonium centres in GaAs and GaP are all deep states. Various aspects of muonium studies in an important subgroup of this family, the III–V nitrides, are covered in an accompanying paper [20]. InN provides an example of a shallow state in a semiconductor of quite small bandgap (the recently revised bandgap is 0.2 eV [24]) and contrasts sharply with a quasi-atomic muonium state lately reported in InSb [25], for which the bandgap is even smaller. In both families of material, therefore, II–VIs and III–Vs, the competition or switch between deep and shallow states is remarkable; it reflects an instability of the electronic structure of interstitial muonium and, by inference, of hydrogen [6].

For shallow-donor states of muonium, it is the interstitial positive muon, of course, which plays the role of charge defect. The unpaired electron should then move with the effective mass of a conduction electron in an orbital which is additionally dilated by the bulk dielectric constant of the medium. This is the effective-mass approximation, in which the binding energy and orbital radius are independent of the chemical nature of the impurity or dopant, given by the standard expressions [11, 12]:

$$R^* = R_y(m^*/m_e)/\varepsilon^2 \tag{1}$$

and

$$a^* = a_0\varepsilon/(m^*/m_e). \tag{2}$$

The effective Bohr-radius a^* and correspondingly dilated 1s wavefunction are envisaged as defining an envelope function or wavepacket of conduction band states—in practice a superposition of cation orbitals in these ionic materials, e.g. 4s(Zn) in ZnO or 5s(Cd) in CdS, etc. This is sketched in figure 1(c). As an example, in ZnO the electron effective mass is $m^* = 0.24\ m_e$ and the dielectric constant is $\varepsilon(0) \approx 8$ (it is the static, not the high-frequency permittivity which is relevant here), giving a binding energy from equation (1) of close to 50 meV. This compares favourably with most of the reported ionization energies: a detailed critique and discussion of the relationship with donor depth is given elsewhere [6]. We return to the implications for the hyperfine constant below, noting here simply that equation (2) implies an electronic orbital spreading well out onto the surrounding lattice, with a characteristic radius

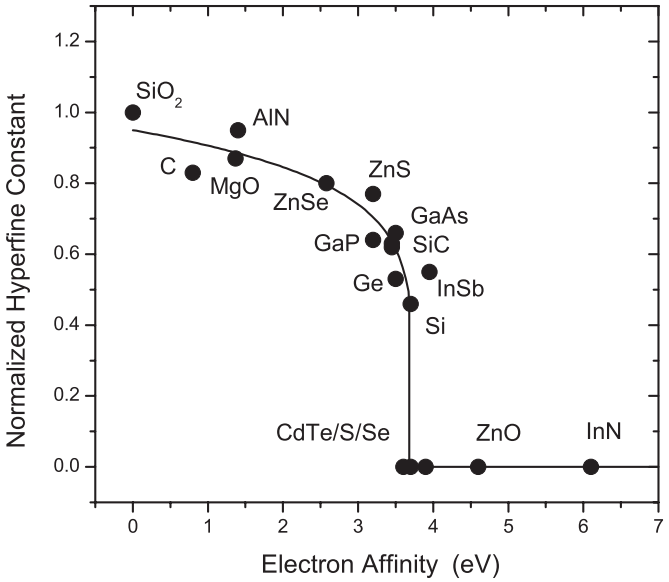

Figure 2. Variation of muonium hyperfine constant with electron affinity [6, 32] (including the new data for InSb [25]), illustrating the deep-to-shallow transition.

of the envelope function in ZnO of

$$a^* \approx 33\, a_0 = 18\ \text{nm}. \tag{3}$$

The question of whether hydrogen itself forms deep or shallow defect centres is a matter of some practical importance, since as a deep-level defect it compensates deliberate dopants, opposing the desired conductivity, but as a shallow donor it could act as a dopant in its own right, inducing n-type conductivity [26]. Various theoretical works address this issue and identify electron affinity as the controlling parameter of the host material [27–29]. So far, only in ZnO has a neutral (undissociated) shallow-donor state of hydrogen been identified spectroscopically, namely by a combination of ESR and ENDOR spectroscopy [30], but both in this material and in InN the role of hydrogen in inducing n-type conductivity has long been suspected from electrical measurements. Both for the shallow and deep states, therefore, muonium data are more comprehensive and provide the better picture of the systematics. The situation is summarized in figure 2, where it appears that the quasi-atomic muonium states dilate progressively with increasing electron affinity, up to a critical value near 3.5 eV, beyond which the electron delocalizes into a diffuse packet of conduction-band states [6, 32]. Different criteria evidently apply to the formation of anomalous muonium, probably related to a degree of sp^3 hybridization and directional bonding which was an essential ingredient of the original bond-centre model [7].

2. Compact versus extended orbitals

This brings us to the questions which the experiments described in the remainder of this paper are designed to test. For the shallow-donor candidates, is the low value of the muon contact interaction really due to the overall extension of the electron wavefunction, as in figure 1(c), or could it represent a nodal point of a more compact orbital, as in figure 1(b)? For the purposes of estimating hyperfine constants in the effective-mass model, it has so far been assumed [6, 16]

that the same envelope function relates the occupancy of 1s(Mu) at the central muon site to that of 4s(Zn) or 5s(Cd) on neighbouring cation nuclei. This implies a contact hyperfine interaction which is reduced from the free-muonium value of 4.5 GHz by a factor $(a_0/a^*)^3$. (Roughly speaking, central spin density is reduced by the volume ratio.) Again taking ZnO as an example, equation (3) gives the reduction factor as 1/36 000, predicting a contact term which is close to but in fact somewhat smaller that the measured value of 0.5 MHz. The argument fails entirely if the picture of a single envelope function is unfounded. The hyperfine parameters reported for the shallow state in GaN [21], taken literally, even imply a *negative* contact interaction at the muon, as though spin-polarization of the valence electrons gives a greater contribution at the muon site than the density of the singly-occupied orbital.

The question would be answered unequivocally by measurement of the superhyperfine interactions on the adjacent nuclei, i.e. by a direct mapping of the local (electron) spin-density distribution anticipated in figure 1(c). However, nuclear magnetism is weak in the II–VI compounds so that, in natural isotopic abundance, only 4% of zinc nuclei (^{67}Zn) and 25% of cadmium nuclei (^{111}Cd and ^{113}Cd) carry dipolar moments. Weak features in a ^{67}Zn ENDOR spectrum have been assigned to near neighbours of the hydrogen shallow donor [30]; the maximum detected splittings are just over 1 MHz and would correspond to spin densities on the nearest Zn nuclei of about 0.05%, the atomic coupling for 4s(^{67}Zn) being 2 GHz [31]. So far, however, no resolved level-crossing resonances that can be used to calibrate the nearest-neighbour or next-nearest neighbour interactions have been reported for the muonium centre. (We have ourselves searched carefully with field scans up to 50 mT both in CdS and in ZnO [33].) Longitudinal-field measurements reveal only a characteristic low-field decoupling of the superhyperfine interactions, observed as a monotonic suppression of cross-relaxation rate with increasing field, albeit broadly consistent with the expected distribution of values [34].

We have therefore resorted to a study of the electron g-factors as a means of distinguishing compact and extended electron orbitals. This is the parameter which controls the ESR frequency $\nu_e = \frac{1}{2\pi}\omega_e$—and hence the electron Zeeman energy term $\hbar\omega_e$ in the spin Hamiltonian for a paramagnetic centre—according to the usual expression

$$\hbar\omega_e = g\mu_B B \tag{4}$$

(with μ_B equal to a Bohr magneton and B the magnetic field). For free atomic muonium in its 1s ground state, the electron g-factor takes its spin-only value, $g_e = 2.0023$. The approximation $g_e = 2.00$ will do for our purposes. Values reported in the early literature for normal (i.e. quasi-atomic) muonium in diamond, Si, Ge, GaP, GaAs, ZnS, ZnSe, etc all lie within 1% of this spin-only value [3]; thus, even for LCAOs of the type sketched in figure 1(a), the orbital contribution is negligible. For bond-centred muonium, the strong anisotropy of the hyperfine tensor prompted a deliberate search for anisotropy of the g-factor in Si and Ge but, again, all deviations from the free-electron value proved to be less than 1% [3]. One can say that, for compact centres even of the molecular orbital type, orbital angular momentum is quenched and spin–orbit coupling is low. The tightly bound electrons have no conduction-electron character[7].

For shallow-donor states, on the other hand, the extended orbital sketched in figure 1(c) may be considered as a wavepacket of conduction-band states [11, 12]. For these latter, spin–orbit coupling is by no means negligible and the departure from free-electron g-factors can be considerable. We do not use the formula explicitly but a useful approximation [36], relating

[7] This argument cannot strictly be made for Si, where conduction electrons in any case have a g-factor close to 2; it holds well for GaAs and Ge, however, where the conduction-electron values are respectively −0.44 and −3.0 [35].

Table 1. Experimental electron g-factors for muonium states in the relevant II–VI compounds, compared with respective literature values [37–41] of shallow-donor electrons.

Sample	$\|g\|$ (this work)	Shallow-donor g^* (literature value)
ZnO	1.97 ± 0.01	1.96
CdS	1.86 ± 0.02	1.78
CdSe	0.505 ± 0.02	0.67
CdTe	1.675 ± 0.025	−1.59

g-factor to electron effective masses, is (with spin orbit coupling Δ and band gap E_g)

$$g^* \approx 2 - \left(\frac{2\Delta}{3E_g + 2\Delta}\right)\left(\frac{m_e}{m^*} - 1\right).$$

Invariably, g^* is less than 2 for donors and greater than 2 for acceptors, according as to whether orbital states which lie higher or lower in energy in the band structure contribute. Note that for donors, g^* can even take on negative values (i.e. a reversal of the sense of the precession, as is the case in CdTe). Table 1 gives literature values for shallow-donor dopants or chemical impurities in some of the II–VI compounds; the necessary sensitivity of the measurement was mostly achieved by the use of ODMR (optically detected magnetic resonance) [37–41].

3. Principle of the measurement

The muon spin rotation spectrum for the shallow paramagnetic state shows a pair of lines centred around the Larmor precession frequency. (The central line is invariably present in the spectrum, representing electronically diamagnetic muons in the sample or its holder.) In sufficiently high fields the electron eigenstates are either spin-up or spin-down with respect to the applied field. The two satellite lines therefore correspond to spin transitions of the muon alone when the electron is either spin-up or spin-down (as is also the case for the nuclear spin transitions in ENDOR spectra). The frequencies and amplitudes of these muon signals are (to a very good approximation) independent of the splitting between electron spin-up and spin-down states and so are not themselves sensitive to g in this régime. Their separation is given, in frequency units, by the muon–electron hyperfine constant A, it being a sufficiently good approximation for the present purposes to assume an isotropic or scalar hyperfine coupling of the form $hA\mathbf{I}.\mathbf{S}$. (A small anisotropy of the interaction is in fact apparent, as may be seen in figure 3 below, where it is the main cause of the broadening and characteristic lineshapes of the transverse-field (TF) μSR spectrum; the appropriate expressions for the explicit angular dependence are given and discussed elsewhere [6].)

If we apply a radio-frequency (RF) magnetic field at a frequency corresponding to a transition between an electron spin-up and spin-down state, we can probe this energy difference (equation (4)). Low RF power induces transitions between specific levels. The resulting TF μSR spectrum will show slow relaxation or splitting of both lines when on resonance. This is similar to the so-called DEMUR (double electron–muon resonance) effects observed in quartz [42] and silicon [43]. Either the frequency or the field may be swept through resonance to plot out the line. If there is any inhomogeneous broadening of the electron splitting, these lines will be broadened and weakened, the area remaining constant.

High RF power has a different effect. We define high power as $g\mu_B B_1/h > A$ so that the electron spin is flipped more rapidly than the muon can follow it via the hyperfine coupling. This condition is readily achieved for the putative shallow-donor states, given their

small hyperfine splittings. When on resonance, the hyperfine coupling is then dynamically decoupled or 'motionally averaged' and the muon will appear to be diamagnetic, collapsing the TF spectrum to a single line at the Larmor frequency. For small hyperfine couplings or low statistics, where the two lines are not resolved, the effect is to reduce the overall relaxation or damping of the TF time-domain signal, i.e. to reduce the rms width of the frequency spectrum. The electron resonance defined by equation (4) may be inhomogeneously broadened (we include here additional hyperfine couplings to other nuclei); only those electrons on resonance are decoupled from the muon and the effect is to reduce the amplitude of the paramagnetic lines and increase the amplitude of the diamagnetic signal. The line has a 'power broadened' width B_1, however, so that B_1 can usually be made large enough to match the inhomogeneous broadening and so observe an intense resonance line.

The resonance frequencies used are actually quite low compared to most ESR experiments—typically 50–120 MHz, with muon precession in the range 0.25–0.6 MHz.

A similar resonant decoupling of the muon and electron can be observed in longitudinal geometry, i.e. with the static field along the initial muon polarization (in our case in-line with the muon beam). In this case it is necessary to measure close to the 'level crossing' field $\frac{1}{2\pi}\gamma_\mu B_0 = \frac{1}{2}A$ where (in the absence of an RF field and due to anisotropic but time-independent terms in the hyperfine interaction) the muon's polarization is reduced by admixture with the electron spin states. Applying RF power at the electron's Larmor frequency will decouple it from the muon and thus *increase* the observed muon polarization—again making the muon state appear diamagnetic. The result is a remarkable resonant *repolarization* [44]. At higher longitudinal field the muon is already fully polarized, so sensitivity to this effect is lost, though in principle a low RF amplitude could cause spin flips of both the electron and muon.

4. Experimental details

We used the MUSR instrument at the ISIS pulsed muon facility [45], in transverse geometry; that is, with the static field B_0 perpendicular to the muon beam. The RF power was provided by a tuned coil with vertically oriented B_1 field, so the initial muon polarization, B_0 and B_1 were all mutually perpendicular. The samples being plate-like single crystals or (for ZnO) thin packages of powder, we used a flat coil of dimensions $30 \times 30 \times 5$ mm^3 with six turns, tuned and matched at the required operating frequency (50–120 MHz). The samples were cooled to typically 5–10 K to observe the shallow-donor states and the resonances displayed at fixed chosen (RF) frequency by scanning the main B_0 field.

The 50 Hz pulsed operation of the ISIS synchrotron allowed particularly efficient use of the RF power, applied in short pulses triggered at each beam pulse: an RF pulse-length of 30 μs covered the entire period of muon implantation, precession and detection at each cycle of the accelerator. A peak RF power of typically 20 W provided a field B_1 of about 1 G but the low duty cycle of the synchronous excitation minimized problems of sample heating. Nonetheless, we measured alternately with RF on and off, routing the data to separate histograms which accumulated simultaneously. This regular switching was sufficiently rapid, typically every 10 s, i.e. every 500 pulses of the ISIS synchrotron, to make the measurements immune to any drifts in field or temperature and ensure that any RF heating of the sample had the same effect on both spectra.

For ZnO, CdS and CdTe, the resonances could be observed clearly as a reduction of the effective hyperfine splitting. In these cases the TF spectra, both with and without RF excitation, were analysed by fitting to three precession signals, with variable splitting and variable amplitude and damping for the outer lines. The frequency of the central 'diamagnetic' line provided a check on the magnetic field calibration. The results for ZnO and CdS have

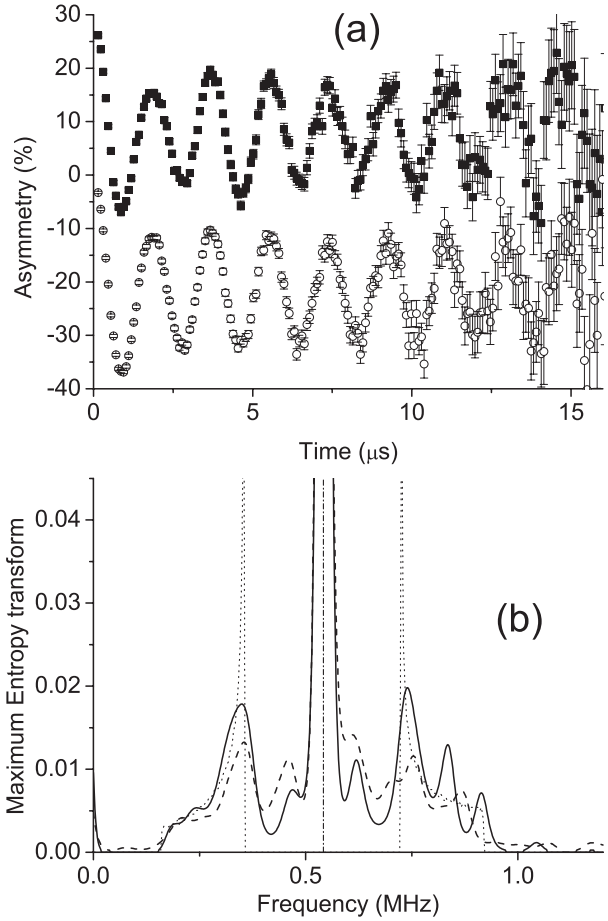

Figure 3. Transverse field muon rotation signal (a) and its transform (b) for the shallow state in ZnO, without RF (■, ——) and with RF on resonance (○, - - - -). The theoretical powder-pattern lineshape [46] is also shown in (b) (· · · · · ·), in its basic form without smoothing of its singularities.

already been reported summarily in a conference proceedings [22]. We reproduce them below together with a similar resonance in CdTe and a demonstration of the resonant-repolarization method for ZnO. For CdSe, where the hyperfine constant is exceptionally low and the splitting less easily resolved, the resonance was more conveniently displayed via the change in rms width σ of the overall spectrum, which we expect to be proportional to A and also dependent on the paramagnetic fraction: in this case we fitted to a single precession line with a Gaussian envelope. The fitted splittings or overall widths were all found to vary somewhat with field (in this low-field range) even with no RF applied, particularly in the Cd compounds. In each case, subtracting the RF-on and RF-off values most clearly reveals the resonances, no further baseline subtraction or correction being necessary.

5. Results

Figure 3 shows typical transverse field spectra and their Fourier transforms, using the maximum entropy technique. These are for a polycrystalline sample of ZnO, so that the hyperfine satellites

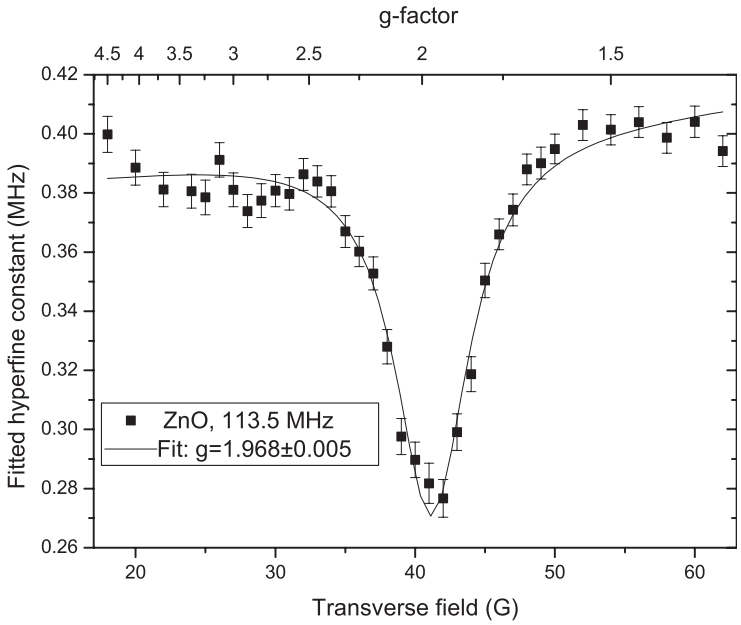

Figure 4. Transverse field scan for ZnO showing the fitted hyperfine constant decreasing when on resonance. An additional Gaussian damping was kept constant.

take on distinctive powder-pattern lineshapes [46]. The difference between RF on and off is visible as an attenuation of the 'beats' in the time domain and corresponding alteration of the satellites in the frequency spectrum. The remaining figures show the indirectly-detected electron spin resonances in all four materials investigated so far by our double resonance methods.

For ZnO a narrow resonance was observed, shown in figure 4. A fitted Lorentzian lineshape gives g close to, but just significantly less than, $g_e = 2.00$. Our value of 1.968 ± 0.005, obtained for a powder sample, is also consistent with the precise principal values $g_\parallel = 1.9569$ and $g_\perp = 1.9552$ obtained by high-field ESR for hydrogen itself in single-crystal ZnO [30]. As a demonstration of principle, resonant repolarization in longitudinal field (LF) was also visible in this material; see figure 5. For CdS, CdSe and CdTe the resonances were considerably broader—probably due to the greater abundance of ^{111}Cd and ^{113}Cd (total 25%) compared to ^{67}Zn (4%)—and only convincingly detected by the TF method (see figures 6–8). For these materials, however, the departure from $g_e = 2.00$ is unmistakable. Importantly, all four g-factors are close to the literature values for known shallow donors in these materials: the comparison is shown in table 1.

6. Concluding remarks

In the absence of a direct mapping of electron density on surrounding nuclei, the present measurements of electron g-factor constitute the best evidence that the singly occupied orbital is spatially extended and may be described by effective-mass theory. In this respect, the new shallow-donor states are qualitatively distinct from the so-called anomalous or Mu* muonium states, where the singly occupied orbital is compact and it is the proximity of a nearby node in the wavefunction that is responsible for the low density at the muon site.

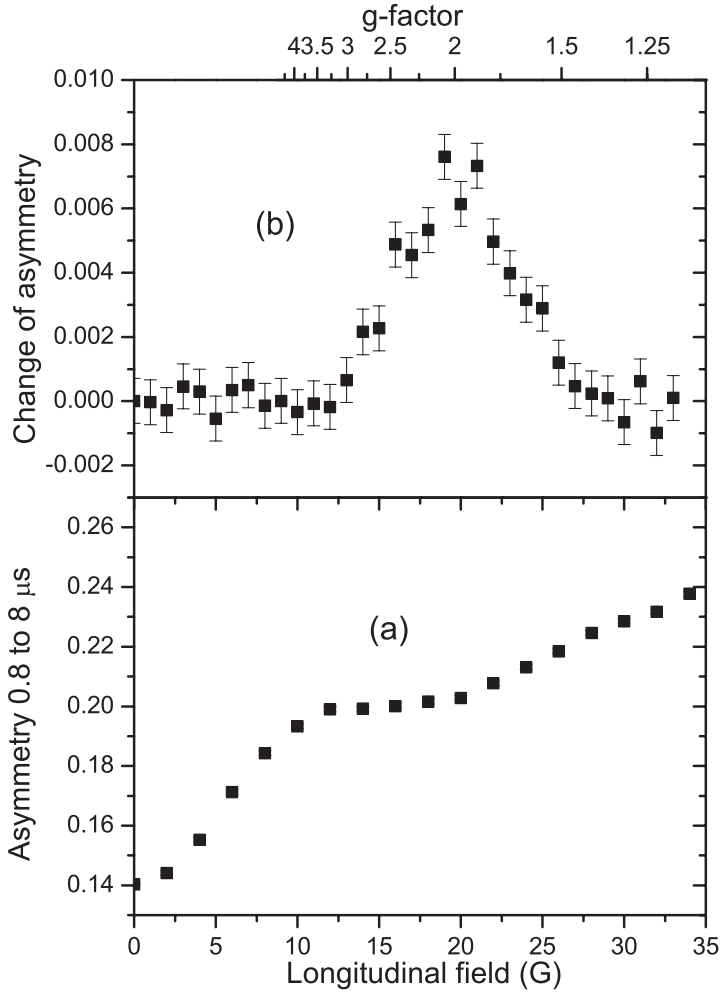

Figure 5. Longitudinal field scan for ZnO showing (a) the repolarization and level crossing in the absence of RF, and (b) the RF resonant repolarization.

In other words, the shallow-donor states differ in kind, rather than degree, from the bond-centred Mu^* states. Since these latter constitute deep donors, it is somewhat surprising that there is not a more gradual evolution or dilation into the shallow donors. But the evidence is clear: the deep-donor Mu^* states have the spin-only g-factor, $g_e = 2.00$, so that orbital angular momentum is fully quenched in these compact states. The new shallow-donor states instead have g-factors reflecting significant, and in some cases dominant, spin–orbit coupling characteristic of conduction-band states: they are essentially identical to those measured for known shallow-donor chemical impurities or dopants. It appears from figure 2 that it is the normal or quasi-atomic muonium states that dilate progressively with increasing electron affinity of the host material, exhibiting a critical transition or switch to the extended states at a threshold around 3.5 eV. This remains to be reconciled with the view of normal muonium as the neutral state of a deep acceptor (converting, either by hole ionization or second electron capture, to the cage-centred negative ion, analogue of the hydride ion, H^-). It does, however, tally with our expectation for these ionic materials that the positive ion resulting from shallow-

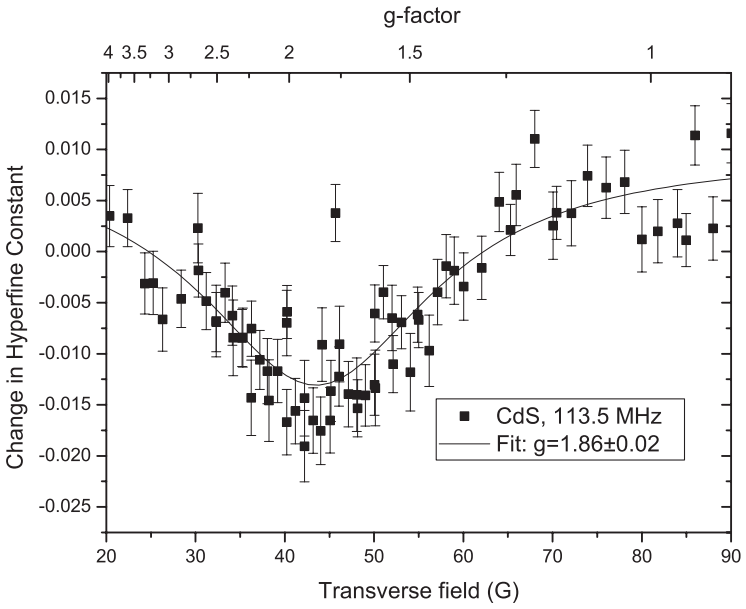

Figure 6. Transverse field scan for CdS showing the change in fitted hyperfine constant on resonance.

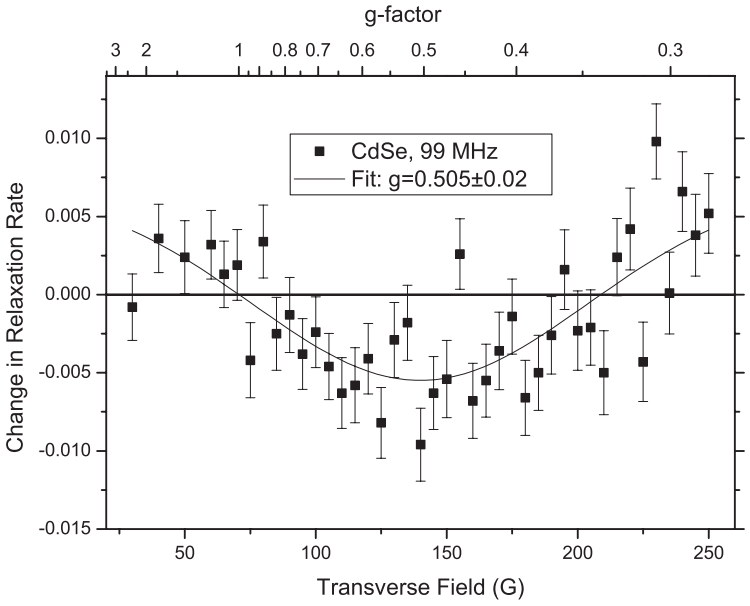

Figure 7. Transverse field scan for CdSe showing the change in Gaussian relaxation rate on resonance.

donor ionization, i.e. the interstitial muon or proton, occupies a cage site antibonding to the anion, rather than the bond-centre site between anion and cation.

As for the possibility of shallow-acceptor states, which might exist for hydrogen and muonium in materials of low work function such as InSb and GaSb [6, 29], it seems doubtful that they would be directly detectable, either by TF μSR or by electron–muon double resonance.

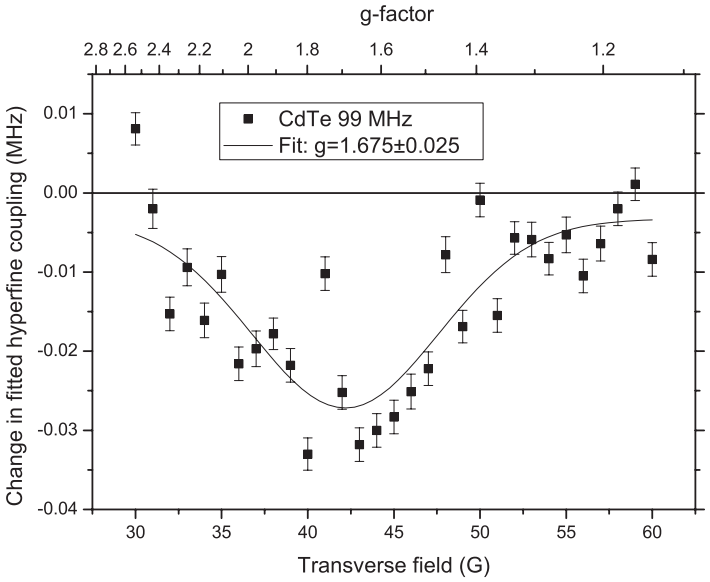

Figure 8. Transverse field scan for CdTe showing the change in fitted hyperfine constant on resonance.

In materials with such a low bandgap as InSb, the shallow-state hyperfine splitting, obscured by nuclear dipolar broadening, is likely to be unmeasurably small. In any case, since states have valence-band (i.e. anion) rather than conduction-band (cation) character, spin–orbit coupling becomes large enough to induce a fierce spin–lattice relaxation. In μSR spectra this would translate as loss of asymmetry, i.e. some degree of prompt depolarization, as we indeed find to be the case for GaSb. (This is not in itself proof of a shallow-acceptor state, however, and it is clear from our measurements that, if such a state is present at low temperature, a deeper quasi-atomic muonium state coexists, persisting almost to room temperature in this material [47].)

The present double resonance study of the II–VI materials ZnO, CdS, CdSe and CdTe is essentially complete, as summarized in table 1. The RF or B_1 field used in these measurements was linearly polarized, so that the B_0-field for resonance determines the magnitude, but not the sign, of the g-factors. Given that the literature value for shallow donors in CdTe is reported as negative [37], it would be of interest to confirm this for muonium, for instance by using a circularly polarized RF field sensitive to the sense of the electron-moment precession. Our resonances are already much broader in the Cd chalcogenides than in ZnO and it remains to be tested whether double resonance could be detected at such low fields in the III–nitride candidates, where nuclear spins are abundant.

It seems likely that shallow-donor hydrogen states exist in other semiconductors or dielectrics, and indeed some predictions have already been made for the broader category of oxide electronic materials [28]. As a method which does not rely on favourable hydrogen solubility for spectroscopic detection, μSR searches for their muonium counterparts look set to play an important role in the initial screening, testing the theoretical predictions.

Acknowledgments

We are indebted to J J Davies, author of several of the ODMR experiments on chemical impurities and shallow dopants [39, 40], for suggesting g-factor measurements on these muonium states, as well as for invaluable discussions.

The work was performed at the ISIS pulsed muon facility under the auspices of EPSRC grant GR/R53067; participation of the Coimbra Group was assisted by FCT/FEDER European Funds (grants POCTI/35334/FIS/2000 and POCTI/43623/FIS/2000—Portugal).

References

[1] Lord J S *et al* 2004 *J. Phys.: Condens. Matter* **16** S4707
[2] Spaeth J-M 1986 *Proc. μSR'86*; *Hyperfine Interact.* **32** 641
[3] Patterson B D 1988 *Rev. Mod. Phys.* **60** 69
[4] ISIS data by this collaboration, with Gil J M, Keren A and Prabhakaran D 2004 *Proc. XIII Int. Conf. on Hyperfine Interactions (Bonn, August 2004)* at press
[5] Cox S F J 2003 *Proc. μSR'03*; *Physica* B **326** 113
[6] Cox S F J 2004 *J. Phys.: Condens. Matter* **15** R1727
[7] Cox S F J and Symons M C R 1986 *Chem. Phys. Lett.* **126** 516
[8] Kiefl R F *et al* 1988 *Phys. Rev. Lett.* **60** 224
[9] Gil J M *et al* 2001a *J. Phys.: Condens. Matter* **13** L613
[10] Cox S F J *et al* 2001a *J. Phys.: Condens. Matter* **13** 9000
[11] Stoneham A M 1975 *Theory of Defects in Solids* (Oxford: Clarendon) (reprinted as an Oxford Classic, 2001)
[12] Standard semiconductor texts: see, for example Yu P Y and Cardona M 1996 *Fundamentals of Semiconductors* (Berlin: Springer)
[13] Hitti B *et al* 1999 *Phys. Rev.* B **59** 4918
[14] Dawson W K *et al* 1997 *Proc. μSR'96*; *Hyperfine Interact.* **106** 97
[15] Gil J M *et al* 1999 *Phys. Rev. Lett.* **83** 5294
[16] Gil J M *et al* 2001b *Phys. Rev.* B **64** 075205
[17] Cox S F J *et al* 2001b *Phys. Rev. Lett.* **86** 2601
[18] Shimomura *et al* 2002 *Phys. Rev. Lett.* **89** 255505
[19] Davis E A *et al* 2003 *Appl. Phys. Lett.* **82** 592
[20] Lichti R L *et al* 2004 *J. Phys.: Condens. Matter* **16** S4721
[21] Shimomura *et al* 2004 *Phys. Rev. Lett.* **92** 135505
[22] Cox S F J *et al* 2002 *Physics of Semiconductors 2002* (*IoP Conf. Series* vol 171) (Bristol: Institute of Physics Publishing) p 69
[23] Vilão R C *et al* 2004 *Phys. Rev.* B submitted
[24] Wu J *et al* 2002 *Appl. Phys. Lett.* **80** 3967
[25] Storchak V G *et al* 2003 *TRIUMF Data* unpublished
[26] Van de Walle C G 2000 *Phys. Rev. Lett.* **85** 1012
[27] Van de Walle C G 2001 *Widegap-2001 (Exeter) and CMMP-2002 (Brighton),* unpublished
[28] Kiliç Ç and Zunger A 2002 *Appl. Phys. Lett.* **81** 73
[29] Van de Walle C G and Neugebauer J 2003 *Nature* **423** 626
[30] Hofmann D M *et al* 2002 *Phys. Rev. Lett.* **88** 045504
[31] Moreton J R and Preston K F 1978 *J. Magn. Reson.* **30** 577
[32] Cox S F J 2003b *Physica* B **340–342C** 250
[33] TRIUMF data by this collaboration, with Lichti R L and Hitti B, unpublished
[34] Lord J S *et al* 2001 *Physica* B **308–310** 920
[35] Madelung O 1996 *Semiconductors—Basic Data* (Berlin: Springer)
[36] Roth L M *et al* 1959 *Phys. Rev.* **114** 90 (equation A-5)
[37] Simmons P E *et al* 1982 *Solid State Commun.* **43** 311
[38] Rössler U (ed) 1999 *Numerical Data and Functional Relationships in Science and Technology* (*Landolt–Börnstein New Series* Group 3, vol 41) Semiconductors XXVI 721
[39] Patel J L *et al* 1981 *J. Phys. C: Solid State Phys.* **14** 1339
[40] Davies J J *et al* 1985 *J. Phys. C: Solid State Phys.* **18** L1035
[41] Block D *et al* 1982 *Phys. Rev.* B **25** 6049
[42] Brown J A *et al* 1983 *Phys. Rev.* B **27** 3980
[43] Blazey K W *et al* 1986 *Phys. Rev.* B **34** 1422
[44] Lord J S *et al* 2003 *Physica* B **326** 128
[45] www.isis.rl.ac.uk/muons/musr
[46] Alberto H V *et al* 2001 *Hyperfine Interact.* **136/137** 471
[47] ISIS data by this collaboration, with Gil J M and Lichti R L 2003 *ISIS Annual Report* RB13814